Long distance measurement with femtosecond pulses using a dispersive interferometer

M. Cui,[1,*] **M. G. Zeitouny,**[1] **N. Bhattacharya,**[1] **S. A. van den Berg,**[2] **and H. P. Urbach**[1]

[1]*Optics Research Group, Department of Applied Sciences, Technical University Delft, The Netherlands*

[2]*VSL, The Netherlands*

[*]*m.cui@tudelft.nl*

Abstract: We experimentally demonstrate long distance measurements with a femtosecond frequency comb laser using dispersive interferometry. The distance is derived from the unwrapped spectral phase of the dispersed interferometer output and the repetition frequency of the laser. For an interferometer length of 50 m this approach has been compared to an independent phase counting laser interferometer. The obtained mutual agreement is better than 1.5 μm (3×10^{-8}), with a statistical averaging of less than 200 nm. Our experiments demonstrate that dispersive interferometry with a frequency comb laser is a powerful method for accurate and non-incremental measurement of long distances.

© 2011 Optical Society of America

OCIS codes: (120.0120) Instrumentation, measurement, and metrology; (320.7100) Ultrafast measurements; (120.3180) Interferometry.

References and links

1. R. Dandliker, K. Hug, J. Politch, and E. Zimmermann, "High-accuracy distance measurements with multiple-wavelength interferometry," Opt. Express **34**, 2407–2412 (1995).
2. B. L. Swinkels, N Bhattacharya, and J. J. M. Braat, "Correcting movement errors in frequencysweeping interferometry," Opt. Lett. **30**, 2242–2244 (2005).
3. D. Jones, S. A. Diddams, J. K. Ranka, A. Stentz, R. S. Windeler, J. L. Hall, and S. T. Cundiff, "Carrier-envelope phase control of femtosecond mode-locked lasers and direct optical frequency synthesis," Science **288**, 635–639 (2000).
4. K. Minoshima and H. Matsumoto, "High-accuracy measurement of 240 m distance in an optical tunnel by using of a compact femtosecond laser," Appl. Opt. **39**, 5512–5517 (2000).
5. J. Lee, Y.-J. Kim, K. Lee, S. Lee, and S.-W. Kim, "Time-of-flight measurement with femtosecond light pulses," Nat. Photonics, **4**, 716–720 (2010).
6. J. Ye, "Absolute measurement of a long, arbitrary distance to less than an optical fringe," Opt. Lett. **29**, 1153–1155 (2004).
7. M. Cui, M. G. Zeitouny, N. Bhattacharya, S. A. van den Berg, H. P. Urbach, and J. J. M. Braat, "High-accuracy long-distance measurements in air with a frequency comb laser," Opt. Lett. **34**, 1982–1984 (2009).
8. P. Balling, P. Kren, P. Masika, and S. A. van den Berg, "Femtosecond frequency comb based distance measurement in air," Opt. Express **17**, 9300–9313 (2009).
9. Y. Yamaoka, K. Minoshima, and H. Matsumoto, "Direct measurement of the group refractive index of air with interferometry between adjacent femtosecond pulses," Appl. Opt. **41**, 4318–4324 (2002).
10. L. Lepetit, G. Chriaux, and M. Joffre, "Linear techniques of phase measurement by femtosecond spectral interferometry for applications in spectroscopy," J. Opt. Soc. Am. B **12**(12), 2467–2474 (1995).
11. K.-N. Joo and S.-W. Kim, "Absolute distance measurement by dispersive interferometry using a femtosecond pulse laser," Opt. Express **14**, 5954–5960 (2006).

#138705 - $15.00 USD Received 23 Nov 2010; revised 24 Dec 2010; accepted 18 Jan 2011; published 23 Mar 2011

12. K. N. Joo, Y. Kim, and S. W. Kim, "Distance measurements by combined method based on a femtosecond pulse laser," Opt. Express **16**, 19799–19806 (2008).
13. I. Coddington, W. C. Swann, L. Nenadovic, and N. R. Newbury, "Rapid and precise absolute distance measurements at long range," Nat. Photonics **3**, 351–356 (2009).
14. Y. Salvade, N. Schuhler, S. Leveque, and S. Le Floch, "High-accuracy absolute distance measurement using frequency comb referenced multiwavelength source," Appl. Opt. **47**, 2715–2720 (2008)
15. S. Hyun, Y. J. Kim, Y. Kim, J. Jin, and S,-W. Kim, "Absolute length measurement with the frequency comb of a femtosecond laser," Meas. Sci. Technol. **20**, 095302 (2009).
16. U. Schnell, E. Zimmermann, and R. Dandliker, "Absolute distance measurement with synchronously sampled white-light channelled spectrum interferometry," Pure Appl. Opt. **4**, 643–651 (1995).
17. M. Takeda, H. Ina, and S. Kobayashi, "Fourier-transform method of fringe-pattern analysis for computer-based topography and interferometry," J. Opt. Soc. Am. **72**, 156–160 (1982).
18. C. Dorrer, N. Belabas, J. P. Likforman, and M. Joffre, "Spectral resolution and sampling issues in Fourier-transform spectral interferometry," J. Opt. Soc. Am. B **17**, 1795–1802 (2000).
19. K. P. Birch and M. J. Downs, "Correction to the updated Edlén equation for the refractive index of air," Metrologia **31**, 315–316 (1994).
20. C. Dorrer, "Influence of the calibration of the detector on spectral interferometry," J. Opt. Soc. Am. B **16**, 1160–1168 (1999).
21. A. Bartels, D. Heinecke, and S. A. Diddams, "Passively mode-locked 10 GHz femtosecond Ti:sapphire laser," Opt. Lett. **33**, 1905–1907 (2008)
22. R. Paschotta, A. Schlatter, S. C. Zeller, H. R. Telle, and U. Keller, "Optical phase noise and carrier envelope offset noise of mode locked lasers," Appl. Phys. B **82**, 265–273 (2006).
23. D. W. Rush, P. T. Ho, and G. L. Burdge, "The coherence time of a modelocked pulse train," Opt. Commun. **52**, 41–45 (1984).

1. Introduction

Optical interferometry is a key technology for accurate absolute length measurement, ranging from the nm scale (e.g. measuring the displacement of a scanning probe microscope) to the km scale (e.g. long baseline interferometry). An important parameter in interferometry is the range of non-ambiguity. In order to deal with the ambiguity, interferometric length measurements are either incremental, or a-priori knowledge of the distance to be measured is required. For single wavelength interferometry the range of non-ambiguity is determined by the wavelength of the source. However, in many cases the a-priori knowledge of the distance to be measured is not known within a single wavelength and thus insufficient for unambiguous length determination. Since incremental measurement (based on fringe counting and phase interpolation) is often not possible, several techniques have been developed to increase the range of non-ambiguity. These techniques include multiple wavelength interferometry [1] and frequency sweeping interferometry [2].

With the advent of the femtosecond frequency comb [3] a new tool for distance measurement has become available. The frequency comb can be considered as a multi-wavelength source, emitting tens of thousands phase-locked wavelengths simultaneously, that together add up to a pulse train of femtosecond pulses. The synthetic wavelength of this source is equal to the distance between the emitted pulses, which is in the order of 1 m. Since the synthetic wavelength determines the range of non-ambiguity, the requirement on a course pre-measurement are rather loose and can be easily fulfilled with alternative methods like time-of-flight measurement. This makes the frequency comb a promising source for for highly accurate, non-incremental and absolute long distance measurement [4, 5]. Several measurement schemes for comb-based distance measurement have been proposed and implemented, exploiting the special properties of the comb: a fixed pulse to pulse phase relation, a broad spectrum and a long coherence length. Some schemes are either based on correlation measurement [6–9] or dispersive interferometry [10–12]. Other schemes exploit two combs [13], use the comb as a reference for multi-wavelength interferometry [14] or frequency sweeping interferometry [15].

In 2009, we experimentally demonstrated that a femtosecond laser can be used for long

#138705 - $15.00 USD Received 23 Nov 2010; revised 24 Dec 2010; accepted 18 Jan 2011; published 23 Mar 2011
(C) 2011 OSA

distance measurement by detecting the cross correlations formed in a Michelson interferometer. The measurements showed an agreement within 2 μm in comparison to a counting laser for a measured distance of 50 m [7]. Due to the dispersion of air, the whole power spectral density (PSD) of the comb has to be measured accurately to predict the shape of the cross correlation function. This shape can be seriously chirped when one arm of the interferometer is much longer than the other. Moreover, the measurement of correlation functions requires the periodic movement of one of the interferometers over a calibrated distance.

In order to overcome some of these disadvantages, dispersive (or spectral) interferometry may be applied. Instead of measuring cross correlations, the interferometer output is dispersed and interfered spectrograms are measured. The distance is determined from the unwrapped phase of the spectrogram [11]. This is strongly related to white light interferometry with dispersive interferometers, that has already been used widely before the advent of ultrashort pulse lasers [16]. When using phase-coherent pulses, however, interferometry is not only possible for interferometers with almost equal path-lengths, but also for path-length differences close to multiple of the inter-pulse distance.

In this paper we apply frequency-comb based dispersive interferometry for measuring a distance of 50 m (100 m total path length) in air. In our measurement scheme we introduce a new calibration approach, which abandons the need of full spectral calibration of the spectrometer. We further point out that, using this technique, the knowledge of the entire PSD of the source is not needed, but only one arbitrary frequency within the range of the comb spectrum is needed for extracting the distance information. Another advantage of this scheme is that, once calibrated, the measurement is performed without moving parts. By comparing to a calibrated counting laser interferometer we find an agreement better than 1.5 μm (3×10^{-8}), with a statistical averaging of less than 200 nm.

2. Measurement principle

In Fig. 1 we show a schematic of the experiment. The beam from the femtosecond pulse laser is collimated into a Michelson interferometer. The output light from both arms is combined and reflected by a diffraction grating. The diffracted beam is then focused by a lens onto a line CCD. Suppose the intensities of the reflected beams from the two arms are equal and the absorption of air can be ignored, the combined spectrum of the two arms is described by equation:

$$S(\omega) = 2|\hat{E_r}(\omega)\cdot\hat{E_m}(\omega)|\left[1+\cos\left(\varphi_r(\omega)-\varphi_m(\omega)\right)\right], \tag{1}$$

where $|\hat{E_r}(\omega)|$ and $\varphi_r(\omega)$ are the electric amplitude and phase of the pulse from the reference arm. $|\hat{E_m}(\omega)|$ and $\varphi_m(\omega)$ are the electric amplitude and phase from the measurement arm. The fundamental property of the interferogram is that it is an intensity measurement that contains the phase difference $\varphi_r-\varphi_m$. This allows the reconstruction of the path-length difference. For a distance propagation in air, the interference term can be written as,

$$\varphi(\omega) = \varphi_r(\omega)-\varphi_m(\omega) = n(\omega)\omega L/c, \tag{2}$$

with n and c being the refractive index of air and the speed of light in vacuum, respectively. The distance L is the geometrical pulse separation between the interfering pulses after the beam splitter.

The experiment is done in the following manner. First, the measurement arm is set such that the path length difference between the two arms is relatively small, but not exactly to zero. At this time a modulated spectrum shown in Fig. 2(a) is observed. Due to the cosine term in Eq. (1), the spectrum is un-distinguishable from its twin image with the same pulse

#138705 - $15.00 USD Received 23 Nov 2010; revised 24 Dec 2010; accepted 18 Jan 2011; published 23 Mar 2011
(C) 2011 OSA

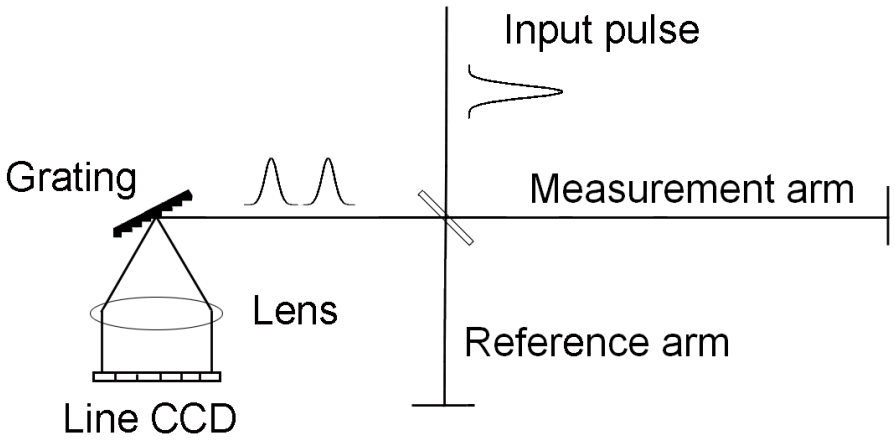

Fig. 1. A schematic to show the measurement principle. The beam from the femtosecond pulse laser is collimated into a Michelson interferometer. The output light from both arms is combined and reflected by a diffraction grating. The diffracted beam is then focused by a lens onto a line CCD.

separation but an opposite sign. This "'twin image"' problem can be solved by moving one arm a little bit and observing how the spectrum changes. While moving the retro reflector in the measurement arm further from the beam splitter, the separation between the two pulses increases and more fringes appear in the measured spectrum. When the number of fringes is beyond the resolution of the spectrometer, the modulation depth becomes shallower, as shown in Fig. 2(b). The fringes disappear when the path length difference between the two arms so large that the number of fringes is much more than the pixel number of the camera, but they reappear when the measurement arm moves about half of the inter-pulse distance because one pulse starts interfering with the next one, as shown in Fig. 2(c). Here $L_{pp}/2$ can be viewed as the synthetic wavelength and spatial overlap between the pulses can always be accomplished when the displacement of the measurement arm is around a multiple of the half inter-pulse distance. The displacement of the measurement arm, Δl, can be written as,

$$\Delta l = m \cdot L_{pp}/2 + L_1/2 - L_2/2, \tag{3}$$

with m an integer and L_{pp} the inter-pulse distance, calculated by $L_{pp} = c/n_g f_r$. Here c is the speed of light in vacuum, f_r is the repetition frequency and n_g is the group refractive index calculated by using the wavelength at the maximum of the power spectral density (PSD) of the pulse. The choice of wavelength for the calculation of n_g will be further discussed in Section 3. Δl is the total displacement of the measurement arm. L_1 and L_2 are the pulse separations before and after the movement of the measurement arm respectively. The signs of L_1 and L_2 are defined as positive when the pulse from the measurement arm is ahead the pulse from the reference arm. The factor two comes from the back and forth propagation. If the jitter of f_r is ignored, the absolute uncertainty of this method should not increase due to increasing the integer number m. This indicates that the maximum distance measured by this technique is only limited by the

#138705 - $15.00 USD Received 23 Nov 2010; revised 24 Dec 2010; accepted 18 Jan 2011; published 23 Mar 2011
(C) 2011 OSA

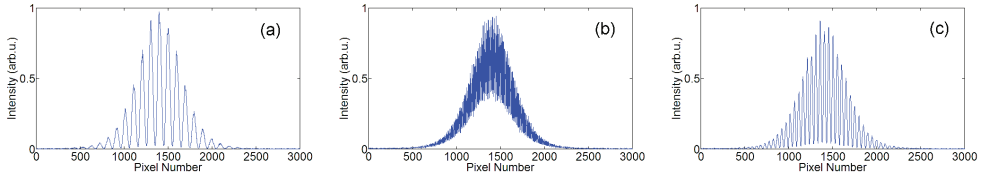

Fig. 2. Spectral interferograms recorded for different pulse separations. (a) Two pulses at a short separation. (b) Two pulses at a large separation. (c) After one cavity length, the fringes re-appear, where one pulse is interfering to its next.

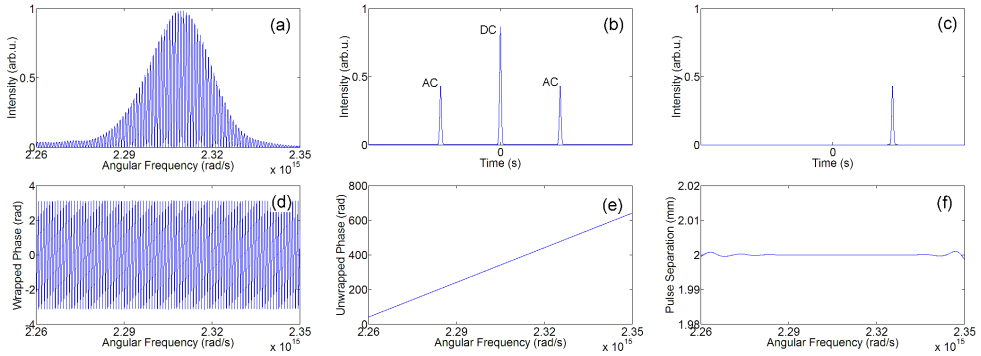

Fig. 3. Data processing procedure for measurement of L. (a) The spectral interferogram *i.e.* dispersed interference intensity captured by the CCD line. (b) Fourier transform of the measured spectral interferogram. (c) The DC peak and one AC peak are band pass filtered. (d) The wrapped phase. (e) The unwrapped phase. (f) The pulse separation obtained from the derivative of the unwrapped phase.

coherence length of the laser source, allowing for low relative uncertainty at long distance. In practice f_r is locked and stabilized within 1 Hz, indicating 1 μm uncertainty in 1 km measured distance. Once the intensity of the spectral interference pattern containing the phase information is recorded, a Fourier filter was used to reconstruct the distance information [11, 17, 18]. The dispersed interference intensity captured by the line CCD is Fourier transformed and shown in Fig. 3(a) to Fig. 3(b). The DC peak is only the power spectral density and contains no phase information. One of the AC peaks is band-pass filtered and inverse Fourier transformed. The phase of the inverse Fourier transform is extracted and from this the unwrapped phase is obtained as shown in Fig. 3(e). Then the distance can be calculated from the derivative of the unwrapped phase,

$$L(\omega) = \frac{c}{n_g}\left(\frac{d\varphi}{d\omega}\right). \tag{4}$$

Here, ω is the angular frequency and n_g is the group refractive index of air. For an unchirped spectral interferogram, L tends to a constant value as shown in Fig. 3(f). In the above equation, $d\varphi/d\omega$ is the derivative of the unwrapped phase, with respect to circular frequency. In order to minimize the uncertainties introduced by Fast Fourier Transform, a zero-padding process and if necessary, a filtering window have to be used to get the best reconstruction.

3. Numerical model for analysis

In order to understand the principle of the spectral interferometer, we simulated the measurement procedure using the PSD of the femtosecond pulses. We first obtained the PSD from the

#138705 - $15.00 USD Received 23 Nov 2010; revised 24 Dec 2010; accepted 18 Jan 2011; published 23 Mar 2011
(C) 2011 OSA

autocorrelation and verified it using an Ocean Optics spectrometer. The frequency at the peak of the PSD is 3.674×10^{14} Hz(816 nm). Using this PSD, the numerical model implemented plane wave propagation at 10^6 individual frequencies, separated by the repetition frequency. The refractive index of air is calculated by the updated Edlén's equation [19]. Spectral interferograms were then calculated using Eq. (1) and Eq. (2).

In Fig. 4(a) we show the spectral interferogram obtained for a path length difference of ±2 mm. The calculated spectral interferogram was analyzed using the procedure described in Fig. 3. The curve shown in Fig. 4(b) shows the derived distance as a function of ω. We can compare this with the distance which we input into the program, *i.e.* 2 mm. We observe that, Fig. 4(b) is mainly a constant at 2 mm, with the oscillations on both sides coming coming from the numerical errors of the FFT.

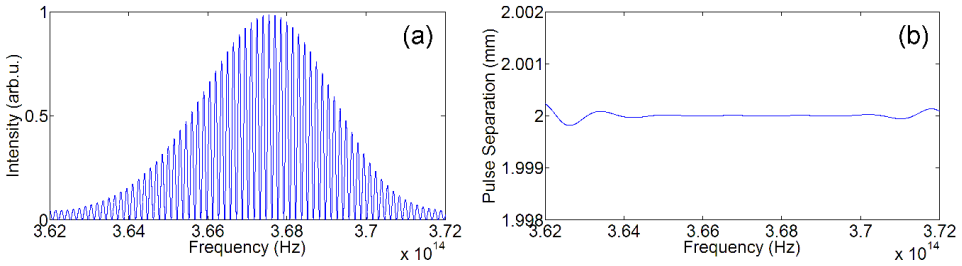

Fig. 4. (a) Numerically simulated interferogram with path length difference equals to $0\times L_{pp}\pm2$ mm. (b) The derived pulse separation as a function of frequency.

In Fig. 5(a) and Fig. 5(c) we show the simulated spectral interferograms for the path length difference of $339\times L_{pp}+2$ mm and $339\times L_{pp}-2$ mm respectively, where L_{pp} is the interpulse distance, calculated by Eq. (5). In our experiments $339\times L_{pp}$ corresponds to a distance of around 100 m. In Fig. 5(a) the fringes are more separated in the high frequency side and the other way round in Fig. 5(c), but these chirps can hardly be seen from the two figures. The chirp is clearly visible in the figures showing the extracted distances, that is Fig. 5(b) for $339\times L_{pp}-2$ mm and Fig. 5(d) for $339\times L_{pp}+2$ mm. An increasing or decreasing derivative of the unwrapped phase always means chirp of the spectral interferogram. Here the twin image ambiguity disappears: A decreasing curve in Fig. 5(b) means the path length difference is shorter than $339\times L_{pp}$. This can be understood by considering that, higher frequency waves propagate slower than lower frequency waves in air. When the path length difference between the two arms is shorter than $339\times L_{pp}$, the pulse reflected from the long arm is in front of the pulse reflected from the short arm. The high frequency component of the pulse from the long arm are closer to the pulse from the short arm. We see that the central region of the curves in Fig. 5(b) and Fig. 5(d) are approximately linear. This is mainly due to the fact that for a small frequency range around 3.674×10^{14} Hz the refractive index of air is approximately a linear function of frequency.

Although the derived distances in Fig. 5(b) and Fig. 5(d) are functions of the frequency, the distance of 2 mm is always shown at the frequency 3.674×10^{14} Hz, as labelled with the dot in both curves. This fact implies that, for deriving the distance information, it is not necessary to know the entire distance curve in Fig. 5(b) but only the small region around 3.674×10^{14} Hz is interesting. The same derived distance of 2 mm in Fig. 5(b) and Fig. 5(d) at 3.674×10^{14} Hz means the fringe densities in Fig. 5(a) and Fig. 5(c) around the frequency 3.674×10^{14} Hz is the same, as labelled by the rectangle. These are the regions that we are interested which contain the distance information.

In an ultrashort pulse, all frequency components propagate with difference velocities. The

#138705 - $15.00 USD Received 23 Nov 2010; revised 24 Dec 2010; accepted 18 Jan 2011; published 23 Mar 2011
(C) 2011 OSA

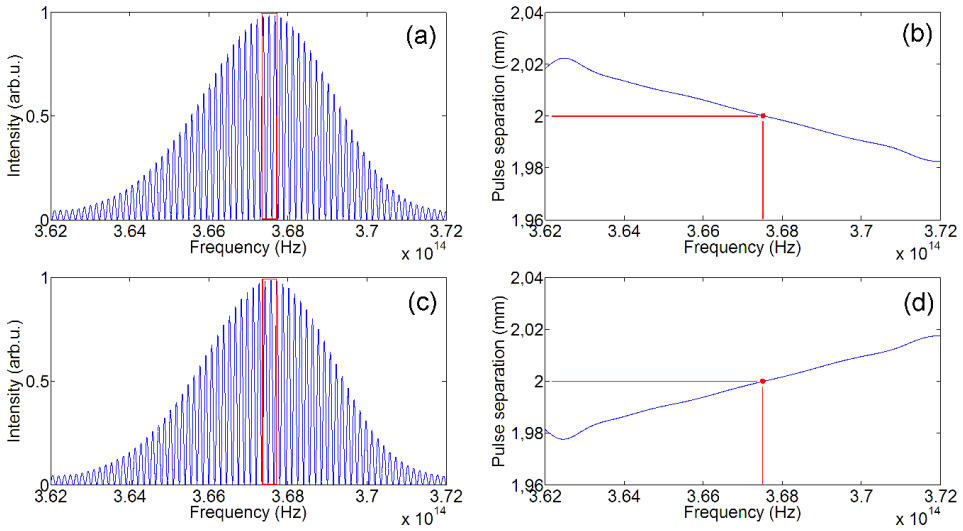

Fig. 5. (a) Numerically simulated interferogram with path length difference equals to $339\times L_{pp}-2$ mm. (b) The derived pulse separation from the spectral interferogram shown in (a). (c) Numerically simulated interferogram with path length difference equals to $339\times L_{pp}+2$ mm. (d) The derived pulse separation from the spectral interferogram shown in (c).

interfered fringes on the spectral interferogram, in a particular region in the frequency domain, can be considered as the interference of this particular frequency component, contained within the pulses reflected from both arms. From the previous paragraph we know that, the distance can be derived from a small region of the spectral interferogram around 3.674×10^{14} Hz. Here 3.674×10^{14} Hz is a special frequency not because it is the maximum of the PSD, but because it is the frequency which we used to calculate L_{pp}. Actually, the exact distance or path length difference which we measure can be extracted from almost the entire curves shown in Fig. 5(b), except for the small regions at the edges which have the numerical artifact due to the Fourier transform. We can choose an arbitrary frequency component in Fig. 5(b), but remember that L_{pp} should also be calculated from the frequency we choose. To illustrate this more clearly, we give an example. Let us select two points from Fig. 5(b), for example, point 1, $f_1 = 3.658\times10^{14}$ Hz $L_1 = 2.009$ mm and point 2, $f_2 = 3.688\times10^{14}$ Hz $L_2 = 1.997$ mm. These two frequencies correspond to two different group refractive indices in air and hence two inter-pulse distances. Using Eq. (5), we have $L_{pp1} = 294.063777$ mm and $L_{pp2} = 294.063742$ mm. The total distance calculated using different frequency components,

$$339\times L_{pp1}-L_1 = 339\times L_{pp2}-L_2 = 99685.611 \quad \text{mm}, \tag{5}$$

is the same.

4. Experimental setup

A schematic of the experimental setup is shown in Fig. 6. A mode-locked Ti:Sapphire laser is the frequency comb source, with both the repetition frequency and the carrier-envelop offset (CEO) frequency referenced to a cesium atomic clock. The pulse duration is 40 fs and the repetition rate is locked at approximately 1 GHz, corresponding to a cavity length of about 15 cm. The CEO frequency is fixed at 180 MHz. The center wavelength of the pulses is 816 nm, with

#138705 - $15.00 USD Received 23 Nov 2010; revised 24 Dec 2010; accepted 18 Jan 2011; published 23 Mar 2011
(C) 2011 OSA

a full width half maximum of about 20 nm. After collimation the beam is sent to a Michelson interferometer. The total power illuminating the interferometer is about 1 mW. One part of the beam is reflected by a hollow corner cube mounted on a translation stage, which forms a short reference arm. The other part of the beam is reflected by two mirrors and propagates along the long measurement arm. One of the mirrors is coated for high reflectivity for near infrared light and high transmission at 633 nm. This was done so that the HeNe fringe counting laser interferometer could be used for a comparison measurement of the measurement arm. The long measurement arm consists of a hollow corner cube mounted on a mechanical car that scans a long rail system of 50 m. A parallel plate is used in the long arm to counter the dispersion of the pulse from the extra transmission from the plate beam splitter. The returning beams are overlapped and focused on a grating spectrometer. The grating spectrometer consists of a slit, a diffraction grating, two achromatic lenses and a line CCD with 3000 pixels. A third gold coated retro reflector on a small translation stage at the beginning of the long arm is added for the reference measurement. A second HeNe fringe counting laser is used to measure the reference arm independently.

5. Measurement procedure

5.1. A new calibration approach

The calibration of the grating spectrometer plays an important role during the distance measurement. First, the pixel number on the line CCD is not necessarily a linear function of wavelength, or, in another word, the angular distribution of the grating output is not linear to the wavelength. Second, in Eq. (4), the derivative of the measured unwarpped phase is with respect to frequency, not wavelength. It is always necessary to convert the x-axis from wavelength to frequency and this conversion leads to unequal x-axis spacing. Thirdly, the wavelength calibration drifts slightly in time due to varying environmental conditions [20]. In our experiment, instead of calibrating the grating spectrometer itself, we measure a short displacement (several millimeters) accurately and use this distance as a reference to measure an unknown distance. In this case, the calibration parameters cancel, but the ratio between the unknown distance and the calibration distance can be calculated from the unwrapped spectral phases obtained from the spectrometer.

For the calibration measurement, the retro reflector mounted on a small translation stage (TS1) at the beginning of the measurement arm was used. During the calibration measurement, TS1 is moved into the beam path and forms a short measurement arm, which is approximately, but not exactly equal to the reference arm. We label the position of the reference arm at this time as ”C1”. A second HeNe fringe counting laser interferometer (HeNe2) is used to measure the reference arm independently. In Fig. 7(a) we show the measured interferogram when the measurement arm is located at position ”C1”. In Fig. 7(b) we show the derivative of the unwrapped phase $d\varphi_{c1}/dx$ obtained from the interferogram in Fig. 7(a), with respect to the pixel number x. Please notice $d\varphi_{c1}/dx$ is not a constant. We can assume that the relation between the pixel number x of the CCD line camera and the circular frequency ω follows an arbitrary relation,

$$x = \Omega(\omega), \tag{6}$$

where x spans from 1 to 3000 pixels in our experiments. Substituting Eq. (6) into Eq. (4), we get,

$$L = \frac{c}{n_g}\frac{d\varphi}{dx}\Omega^{'}(\omega), \tag{7}$$

where $\Omega^{'}(\omega)$ is the derivative with respect to ω. For a short path-length difference $d\varphi/d\omega$ should be a constant, but $d\varphi/dx$ is related to $\Omega^{'}$. Next, the reference arm is displaced a short

#138705 - $15.00 USD Received 23 Nov 2010; revised 24 Dec 2010; accepted 18 Jan 2011; published 23 Mar 2011
(C) 2011 OSA

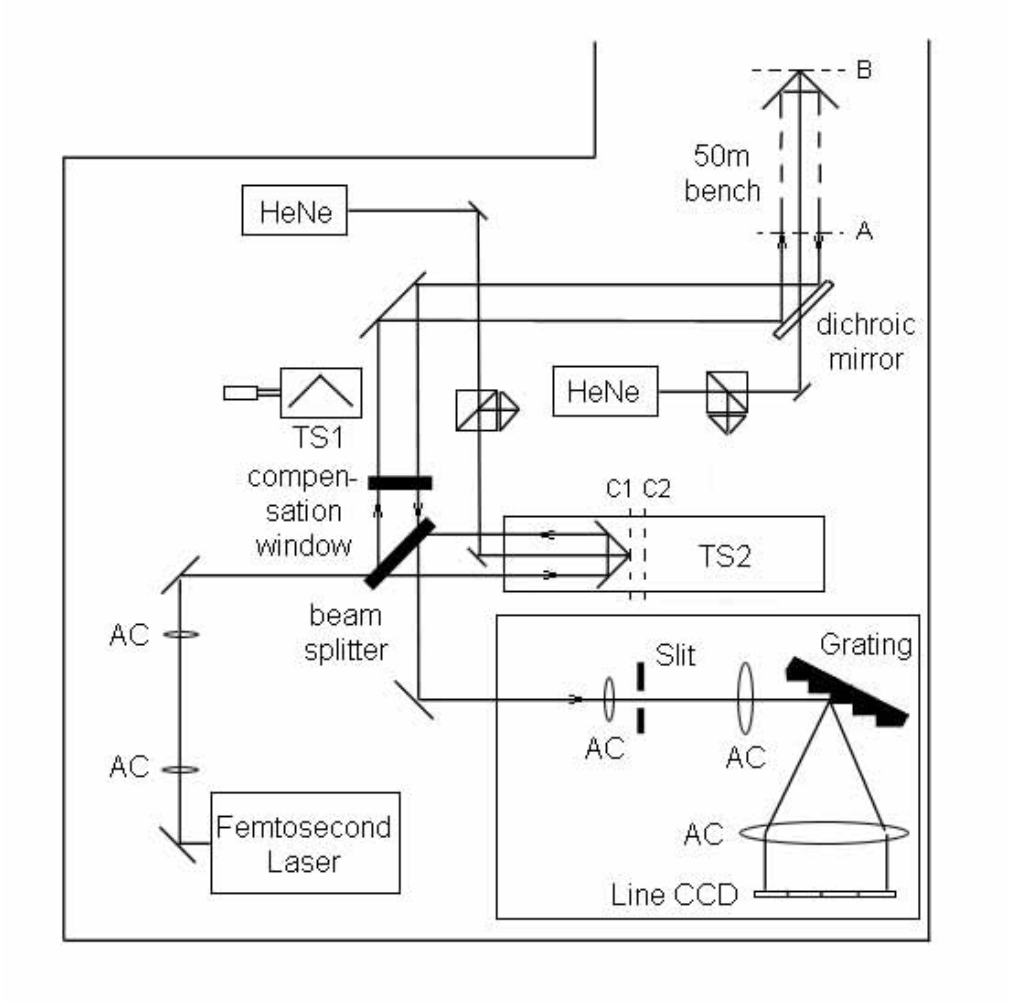

Fig. 6. Schematic of the experimental setup used to measure distances in the 50 m corridor using spectral interferograms. The mode locked Ti:Sapphire laser generates 40 femtosecond pulses with repetition rate of around 1 GHz. The reference arm consists of a hollow corner cube mounted on the translation stage (TS2). The measurement arm consists of two dispersion compensated mirrors and a gold coated retroreflector mounted on a mechanical stage of the 50 m long measurement bench. The HeNe fringe counting laser interferometer was used for a simultaneous comparison measurement. The returning beams were overlapped and focused on a grating spectrometer. A third gold coated retro reflector on a small translation stage (TS1) was added at the beginning of the long arm of the interferometer. A second HeNe fringe counting interferometer was also added to the setup to enable the calibration measurements.

#138705 - $15.00 USD Received 23 Nov 2010; revised 24 Dec 2010; accepted 18 Jan 2011; published 23 Mar 2011
(C) 2011 OSA

distance to position "C2". This displacement is labeled as Δl_c and is simultaneously measured by the second conventional counting laser with an accuracy of 10 nm. The interferogram measured at "C2" is shown in Fig. 7(c) and the derivative of the unwrapped phase $d\varphi_{c2}/dx$ is calculated and shown in Fig. 7(d). Now, the displacement Δl_c is linked to the difference of Fig. 7(b) and Fig. 7(d), or in other words, $d\varphi_{c1}/dx - d\varphi_{c2}/dx$.

$$2\Delta l_c = \frac{c}{n_{gc}} \left(\frac{d\varphi_{c1}}{dx} \Omega'(\omega) - \frac{d\varphi_{c2}}{dx} \Omega'(\omega) \right), \tag{8}$$

where $d\varphi_{c1}/dx$ and $d\varphi_{c2}/dx$ are the derivatives calculated from the unwrapped phase of the modulated spectra as described earlier. n_{gc} is the group refractive index measured at the time of the calibration measurement. Now Δl_c forms the calibration distance. An unknown distance to

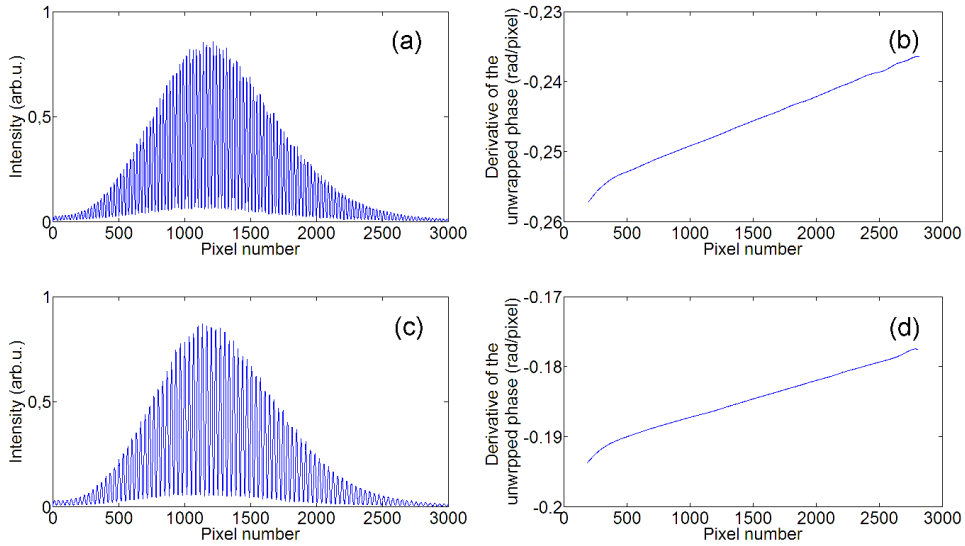

Fig. 7. The spectral interferograms and the derivatives of the unwrapped phases at position C1 and C2 in the calibration measurement. (a) The measured interferogram when the measurement arm is located at position "C1". (b) The derivative of the unwrapped phase $d\varphi_{c1}/dx$ obtained from the interferogram in (a), with respect to the pixel number x. (c) The measured interferogram when the measurement arm is located at position "C2". (d) The derivative of the unwrapped phase $d\varphi_{c2}/dx$ obtained from the interferogram in (c), with respect to the pixel number x.

be measured, L, is linked to Δl_c by,

$$\frac{L}{2\Delta l_c} = \frac{n_{gc}}{n_g} \frac{d\varphi}{dx} \Big/ \left(\frac{d\varphi_{1c}}{dx} - \frac{d\varphi_{2c}}{dx} \right). \tag{9}$$

Here, $d\varphi/dx$ is the derivative of the measured (unknown) unwrapped phase, with respect to x and n_g is the group refractive index at the time of the distance measurement. We observe that the calibration function $x = \Omega(\omega)$ has canceled out. If the environment conditions during the calibration measurement and the long distance measurement is the same, then, the refractive index is also cancelled out.

One common misunderstanding is that, since the measured long distance is obtained by comparing it to the short calibrated displacement, a little error on measuring the calibration distance

#138705 - $15.00 USD Received 23 Nov 2010; revised 24 Dec 2010; accepted 18 Jan 2011; published 23 Mar 2011
(C) 2011 OSA

will be significantly influence the measured long distance. This is not true by considering Eq. (3). The measured distance is dominated by the term $m \times L_{pp}/2$, which is not related to the calibration distance. Only the term L_1 and L_2 is determined from the calibration distance and both of them are less than 3 mm in our experiments.

5.2. Long distance measurement

After the calibration, we translate the retro reflector mounted on TS1 out of the measurement arm. Now the beam is directed to the 50 m bench using two mirrors and the measurement up to 50 m can be performed. The PSD was first remeasured using the grating spectrometer. The maximum intensity appears at pixel number $x = 1150$. By comparing it with the PSD measured with the Fourier transform spectrometer, we know that this corresponds to the frequency of 3.674×10^{14} Hz (816 nm). The measurement is carried out by first placing the mechanical car with the retro reflector, in the long arm, at the closest possible position to the dichroic mirror. The translation stage in the reference arm is scanned and the spectral interferogram is found and recorded. At this time the path length difference between both arms is around 1.5 m, corresponding to 9 times of the cavity length. Let us label the position of the measurement arm at this position of the retro reflector as A and the distance between the two interfering pulses as L_A. In Fig. 8(a) we show a typical measured spectrum at this position. Then the modulated spectrum is analysed and the derivative of the unwrapped phase $d\varphi_A/dx$ is plotted in Fig. 8(b). This curve is compared to the curves during the calibration, Fig. 7(b) and Fig. 7(d) by using Eq. (9) and the derived pulse separation is shown in Fig. 8(c). The derived separation between the interfered pulses is almost a constant, implying that at short path-length difference the chirp of the pulse can be ignored. Subsequently for each measurement the mechanical car

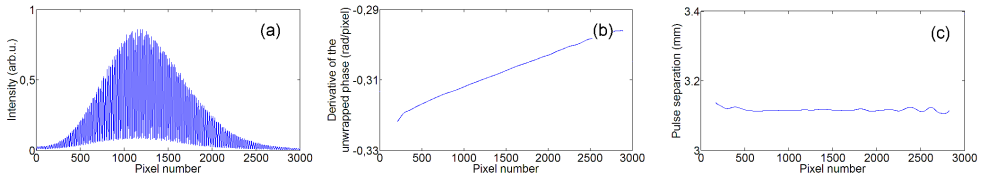

Fig. 8. (a) A typical measured spectral interferogram at the beginning of the bench and the derived distance as a function of pixel number. (b) The derivative of the unwrapped phase. (c) The derived pulse separation after calibration.

was moved over a long distance which we label as position B. This long distance is around 50 m, corresponding to 339 times the cavity length. At this time the distance between the two interfered pulses is L_B and a new spectral interferogram is recorded. One such spectral interferogram is shown in Fig. 9(a). The reflected beam drops considerably in power, leading to a drop in the modulation depth, but the fringes were clearly visible. The derived pulse separation after calibration is shown in Fig. 9(c). At pixel number $x = 1150$ the read out of the distance $L_B = 0.9455$ mm. The derived pulse separation is decreasing respected to wavelength. This means the path length difference is $339 \times L_{pp} + 0.9455$ mm. The turbulence in air causes the fringes in the spectral interferogram to vibrate, which can be seen in the corresponding curve in Fig. 9(c). This leads to an uncertainty of around 2 μm. The measured spectral interferogram and the derived pulse separation are also compared with simulation. Fig. 9(b) is the simulated spectral interferogram for this distance. To give a good comparison, the x-axis of Fig. 9(b) was chosen to be the wavelength, and the power of the reflected beam was taken to be only $1/10$ of the original. The pulse separation calculated from the simulation is shown in Fig. 9(d). Besides the aliasing on both sides, the central parts of (b) and (d) match quite well, as indicated by the

#138705 - $15.00 USD Received 23 Nov 2010; revised 24 Dec 2010; accepted 18 Jan 2011; published 23 Mar 2011
(C) 2011 OSA

red line in Fig. 9-(c).

We also give an example when the path-length difference between the two arms is shorter than $339 \times L_{pp}$. Fig. 10(a) and Fig. 10(c) show the spectral interferogram and the derived pulse separation at $L_B = -2.9228$ mm. The spectral interferometer and the derived curve of the pulse separation is also compared with the simulations, as shown in Fig. 10(c) and Fig. 10(d). The total displacement of the measurement arm is calculated from Eq. (3), where L_{pp} is calculated by $L_{pp} = c/n_g f_r$ and n_g is the group refractive index of air at 3.674×10^{14} Hz (816 nm).

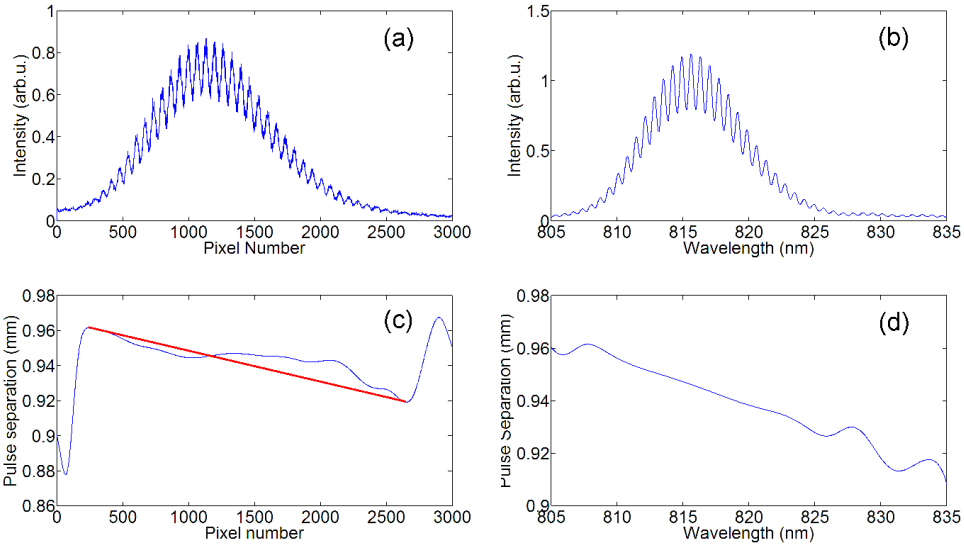

Fig. 9. (a) A typical measured interferogram with path length difference longer than $339 \times L_{pp}$. (b) The simulated spectral interferogram using $L = 0.9455$ mm. (c) The derived pulse separation from the measurement data in (a). At pixel number $x = 1150$ the read out of the distance $L = 0.9455$ mm. The decreasing slope of the curve indicates a positive sign. (d) The pulse separation calculated from the simulation using $L = 0.9455$ mm.

5.3. Measurement Result

During the measurement, the fluctuation of the temperature in the laboratory was controlled to be less than 0.1 °C. The pressure and humidity have been monitored with an accuracy of 1 hPa and 1% respectively. The calibration distance of around 3 mm was used. Each time the translation stage was displaced from pulse separation of -1.5 mm to pulse separation of +1.5 mm., This process is repeated 6 times independently and the averaged calibration distance was used. Totally 5 groups of long distance measurement were performed. We chose different f_r for each group. Within each group 6 independent measurements were performed. In each measurement, we arbitrarily chose L_1 and L_2 in Eq. (3). At each position the spectral interferogram is recorded 5 times to statistically minimize the uncertainty. One 50 m measurement took about 10 minutes, mostly occupied by transporting the retroreflector down the 50 m bench. The measured displacement is compared with measurement of the HeNe fringe counting laser interferometer and the result is shown in Fig. 11. The agreement in 5 measurements are all within one wavelength, with the standard deviation of around 1 μm. The average of all measurements shows the agreement within 200 nm on 100 m pulse propagation in air, as shown by the dotted line in Fig. 11. We attribute the residual difference and uncertainty in the comparison measurement to vibrations of the setup and air turbulence. The variation and uncertainty of the environmental

#138705 - $15.00 USD Received 23 Nov 2010; revised 24 Dec 2010; accepted 18 Jan 2011; published 23 Mar 2011
(C) 2011 OSA

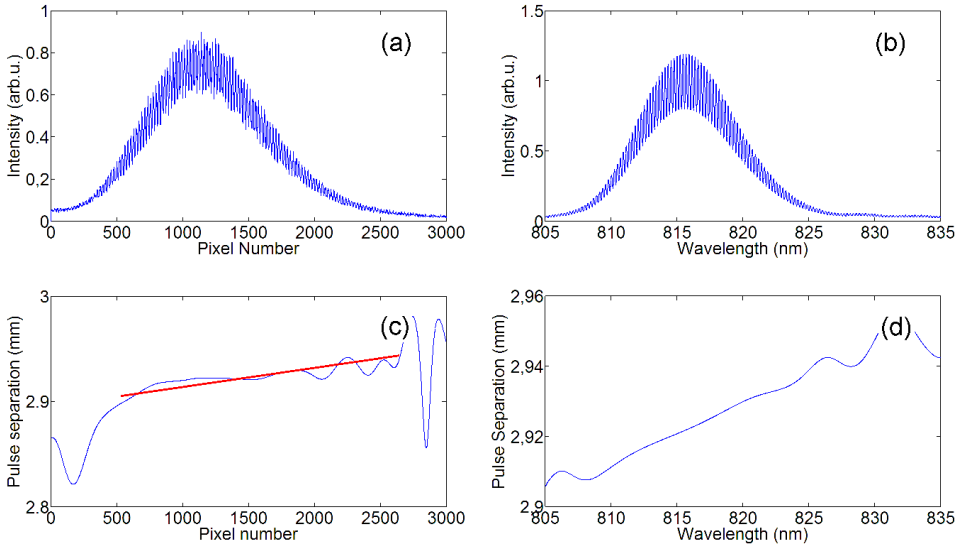

Fig. 10. (a) A typical measured interferogram with path length difference shorter than $339 \times L_{pp}$. (b) The simulated spectral interferogram using $L = -2.9228$ mm. (c) The derived pulse separation from the measurement data in (a). At pixel number $x = 1150$ the read out of the distance $L = 2.9228$ mm. The increasing slope of the curve indicates a negative sign. (d) The pulse separation calculated from the simulation using $L = -2.9228$ mm.

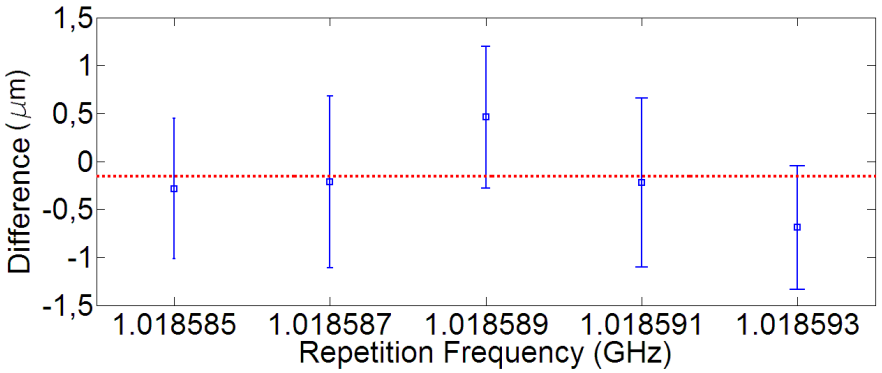

Fig. 11. Comparison measurement of displacements of around 50 m. The error bars indicate the standard uncertainty, derived from measurement reproducibility. The average of all measurements is shown by the dotted line.

#138705 - $15.00 USD Received 23 Nov 2010; revised 24 Dec 2010; accepted 18 Jan 2011; published 23 Mar 2011
(C) 2011 OSA

parameters, limits the accuracy in measuring the absolute distance. For example, a typical uncertainty of 0.1°C in temperature already leads to an uncertainty of the refractive index of air of about 1×10^{-7}, corresponding to 10 μm at 100 m propagation. Also, an uncertainty of 1 hPa in pressure leads to an uncertainty of 2.7×10^{-7}, corresponding to 26 μm at 100 m propagation. Moreover the updated Edlen's equation itself has an intrinsic uncertainty of 1×10^{-8}, implying 1 μm over a path length difference of 100 m. The influences of the environmental parameters on the refractive index at the wavelengths of both the He-Ne laser and the frequency comb cancel in first order. For this is the reason the agreement between the experimental results is much better than 10 μm. The agreement between the frequency comb and the He-Ne laser is much better than the achievable absolute accuracy in air, showing that the measurement result is not limited by the chosen method.

6. Conclusion

In this paper we have experimentally demonstrated that a femtosecond comb laser, combined with a Michelson interferometer and a grating spectrometer can be used for absolute long distance measurement. We have built experimental setups to measure distances up to 50 m using this technique and have shown accuracies of less than 2 μm. If the spectrometer is calibrated, an arbitrary frequency within the frequency comb is needed and the distance can be calculated by using the group refractive index at this particular frequency. In our experiment, we have chosen the frequency at the peak of the PSD. This is not an arbitrary because instead of the spectrum, we calibrated a short displacement. Here, the measured PSD by the CCD line is not calibrated and we have to find a position in the PSD where we know both the actual frequency and the pixel index on the CCD line.

In our measurement, the displacement of the long measurement arm is close to a multiple of the $L_{pp}/2$. This is because in principle our grating spectrometer has the resolution of around 0.04 nm. At this resolution the fringes become hard to distinguish when the distance between the interfered pulses is more than 5 mm. This distance is much shorter than the inter-pulse distance of our femtosecond laser. In order to measure an arbitrary distance, one easy way is to displace the reference arm. There are other solutions for this problem. For example, in 2006, Joo and coworkers suggested the use of an Fabry-Perot Etalon (FPE) before the spectrometer [11]. This filtered some frequencies out of the pulse and reduced the equivalent inter-pulse distance to 2 mm. Another option is to use a frequency comb with a higher repetition frequency [21].

During the measurement, although the temperature, pressure and humidity were monitored, still the variation and uncertainty on the measurement of these environmental parameters, limits the accuracy in measuring the absolute distances. If the experiments are performed in outer space, where the refractive index of air is not needed to be taken into account, then the accuracy of the measurement will be influenced by the noise properties of the femtosecond laser [22], the mechanical vibrations of the experimental setup, the resolution of the grating spectrometer and the calibration of the reference arm. The ultimate maximum distance which can be measured will be limited by the coherence length of the laser source, which depends on the linewidth of the comb lines in the particular comb source. The coherence length of a Ti:Sapphire frequency locked femtosecond laser is of tens of kilometers or more [23]. This is a good property to expect that this method can be applied to measure very long distances, especially in space where the dispersion of air is absent.

#138705 - $15.00 USD Received 23 Nov 2010; revised 24 Dec 2010; accepted 18 Jan 2011; published 23 Mar 2011
(C) 2011 OSA